ELECTRODIFFUSION OF LITHIUM, SODIUM AND HYDROGEN IONS IN SYNTHETIC QUARTZ

By

JERRY DOUG WEST

Bachelor of Science

University of Missouri-Rolla

1980

Submitted to the Faculty of the Graduate College
of the Oklahoma State University
in partial fulfillment of the requirements
for the Degree of
MASTER OF SCIENCE
July, 1984

ELECTRODIFFUSION OF LITHIUM, SODIUM

AND HYDROGEN IONS IN

SYNTHETIC QUARTZ

Thesis Approved:

Joel J. Martin

Thesis Adviser

Timothy M. Wilson

Larry E. Halliburton

Dean of the Graduate College

ACKNOWLEDGMENTS

This thesis was made possible with the help of many people. Foremost is Dr. Joel Martin for his help and expertize in the area of quartz research. I also want to thank my wife and parents for their understanding and support through the long years of my education. Also, I must thank God, who makes all things possible.

This work was supported by the Solid State Sciences Division of the Rome Air Development Command, U.S. Air Force Hanscom AFB.

TABLE OF CONTENTS

TABLE

LIST OF FIGURES

Figure

Page

CHAPTER I

INTRODUCTION

Quartz (SiO_2) is an abundant and useful crystal. Natural quartz can be found in Brazil, Burma, Madagascar and Arkansas. Natural quartz usually has a much higher impurity content than synthetic quartz. These impurities often given natural quartz its' coloration. Depending on the impurities, natural quartz has been given a variety of names by mineralogists, e.g. smoky quartz (aluminum), amethyst (iron), and rose quartz (titanium).

The first synthetic quartz was grown by Spezia [1] in 1908. Presently, synthetic quartz is available in a variety of sizes and impurity concentrations. In today's commerically available quartz the most common substitutional impurity is aluminum. Aluminum which as approximately the same size as a silicon ion, fits nicely into the quartz lattice. A positive interstitial ion is needed for charge compensation at the aluminum defect site. The process of electrodiffusion [2] can be used to diffuse different positive ions to these aluminum defect sites.

Since quartz undergoes a phase transition (from trigonal alpha-quartz to hexagonal beta-quartz) at 573°C [3], it can not be grown from melt. Quartz melts at approximately 1665°C [3]. Nearly all quartz becomes electrically twinned as it is cooled through the 573°C transition temperature. Electrically twinned quartz has only slight atomic

displacements, however, this is enough to rule out its' usefullness for electronic applications.

Synthetic quartz is grown hydrothermally [4]. This process is carried out in an autoclave with two temperature regions. The lower region, which is 5 C° to 30 C° warmer than the upper region, contains crushed quartz. The autoclave is filled with a sodium hydroxide or sodium carbonate solution. The quartz dissolves into solution, then it is transported by convection currents to the cooler upper region where it crystalizes on a seed crystal [4]. Growth temperatures vary from 340°C to 400°C, the pressure is in the range 10^8 to 1.3 x 10^8 Pa (i.e., 15,000 to 20,000 psi). This hydrothermal process is very slow, a useful crystal may take several weeks to grow.

Alpha quartz has a trigonal crystal structure which has no planes of symmetry. Trigonal structures are characterized by an axis of three fold symmetry. This unique axis is called the c axis, or optic axis. Three equivalent two-fold axes (a_1, a_2 and a_3) lie 120° apart in a plane perpendicular to the c axis.

The alpha quartz structure consists of SiO_4 tetrahedra which share each of their corners wtih another tetrahedron. Two of the oxygen ions surrounding the central silicon ion have short bonds (1.606 angstroms), and the other two have long bonds (1.612 angstroms). The angle between oxygen bonds to two adjacent silicon ions is 143.65 degrees. Parallel to the C axis are wide channels of about one angstrom radius. As a result of these channels, ionic transport properties of quartz are very anisotropic. For example, the ionic electrical conductivity is 10^3 higher parallel to the C axis as opposed to perpendicular to it.

Point Defects in Quartz

Point defects are very important in the ionic conductivity of quartz. The concentration of certain defects is directly related to the conductivity [5]. One point defect that is present in nearly all quartz is formed when an aluminun ion substitutes for a silicon in the quartz lattice. The aluminum has a valence of 3, whereas, the silicon has a charge of 4. As a result of this charge difference a positive ion is needed near the aluminum site to compensate for the lack of positive charge. The substitutional aluminum and the positive ion form an electrically neutral defect center. In as-grown quartz alkali ions provide the charge compensation. Electrodiffusion or irradiation replaces the alkali with a proton or with a hole. The concentration of the aluminum is directly related to the growth rate of the crystal [2]. The faster the growth rate the higher the aluminum concentration. These defect centers can be observed in a number of ways. The $Al\text{-}OH^-$ center gives rise to infrared absorption [6,7] peaks at 3306 cm^{-1} and 3367 cm^{-1}. Acoustic loss and dielectric loss [8] is used to measure the $Al\text{-}Na^+$ center. Acoustic loss and electron spin resonance [9] is used to measure the Al-hole center.

Frequently in synthetic quartz the amount of impurity ions measured is in excess of the amount expected to be trapped at the aluminum site. One model proposed by Adams and Douglas [10] has two OH^- molecules at an oxygen site. This double OH defect may account for the excess hydrogen ions in quartz. This model may also account for excess Li^+ or Na^+ when they are attached to the oxygen instead of hydrogen.

Another class of point defects in quartz involve an oxygen vacancy. These centers are known as E' centers [11]. The E' center is an

isolated oxygen vacancy having trapped a single unpaired electron. A closely related center is the E_4' center. The E_4' center consists basically of an H^- ion trapped in the oxygen vacancy with an unpaired electron shared by the two adjoining silicons. At present, the E' centers are not thought to be significantly involved with the electrodiffusion process.

Ionic Conductivity in Quartz

To understand ionic conductivity in quartz [5,12,13] you must first understand the simple case. We assume a crystal with only one type of defect responsible for the ionic conductivity. The motion of the charged ions is effectively one dimensional. In quartz the conductivity is highly anistropic, resulting in a much higher conductivity along the C axis. Associated with each defect is a charge compensating interstitial ion. These ions are said to "hop" between defects resulting in a current. One of the most understood defects in quartz is the substitutional aluminum center [9].

As the temperature is raised more of the $Al\text{-}M^+$ pairs begin to disassociate. This disassociation reaction can be written as

$$(Al - M) \rightarrow Al_s + M_i \tag{1}$$

where M_i denotes the free interstitial alkali and Al_s the unassociated Al^{3+} substitutional.

The conductivity can be written as:

$$\sigma = C_i N_o e \mu_i \tag{2}$$

where C_i is the atom fraction of M_i relative to the S_i atoms, μ_i is the mobility of these interstitials, e is the electronic charge, and N_o is the number per unit volume of S_i atoms in the crystal. The mobility [5] is given by

$$\mu_i = (ed^2/kT)\ \nu_o'\ \exp(-E_m/kT) \tag{3}$$

where d is the jump distance, ν_o' the oscillation frequency, E_m is the activation energy associated with the migration of the ion through the c channel, kT is the product of the Boltzman constant factor and the temperature. From the reaction represented by equation 1 the mass action relation can be written as:

$$\frac{C_i C_s}{C_p} = 1/2\ \exp(-\ E_a/kT) \tag{4}$$

Here C_s is the concentration (in atom fraction) of unassociated substitutionals, C_p is the concentration of $Al\text{-}M^+$ pairs, the factor 1/2 results because the pair has two equivalent orientations, E_a is the activation energy of the Al-M pair. For the temperature regions involved in this experiment most of the M_i ions are associated with aluminum. As a result $C_p >> C_i$ and $C_i = C_s$, C_i and C_s are equal since Al_s and M_i are formed together. The total aluminum concentration C_M is approximately C_p since most of the alkali ions M_i are associated with the aluminum. With these approximations equation 4 can be written as

$$C_i = \frac{C_m}{2} \exp(-\ E_a/2\ kT) \tag{5}$$

By inserting equation 5 and 3 into equation 2, the standard form of the conductivity becomes

$$\sigma T = A \exp[-(E_m + 1/2\ E_a)/kT] \tag{6}$$

where the preexponential factor A is written

$$A = \frac{C_m}{2} N_o e^2 \nu_o' \frac{d^2}{k} \tag{7}$$

In equation 7 ν_o is the least known quantity, it is thought to be about 3×10^{14} Hz. The jump distance d is another quantity which cannot be directly measured. In natural and synthetic quartz this same hoping process is responsible for the ionic conductivity. In real quartz there is more than one type of defect and carrier ion. Another defect that is believed [5,10] to contribute to the conductivity consists of a water molecule attached to an oxygen atom. At present, there are believed to be the two primary conduction mechanisms in quartz.

Since these simultaneous conduction processes act in parallel we can write the conductivity as:

$$\sigma = n_{A\ell} e\mu_{A\ell} + \sum_i n_i Z_i e\mu_i \tag{8}$$

The first term corresponds to the contribution due to the aluminum defect. The second term is due to other defect centers in the quartz.

Purpose of Investigation

The purpose of this work is to investigate the conduction processes

that take place during ionic electrodiffusion of synthetic quartz. The conductivity was measured as functions of temperature and specific ion for three grades of commerically grown quartz. The activation energies for Li^+, Na^+, and H^+ ions were determined. The three grades of synthetic quartz used were Special Premium Q (SP), Premium Q (PQ) and electronic grade (EG). The samples were characterized by infrared absorption measurements of the OH related growth defect bands.

CHAPTER II

EXPERIMENTAL PROCEDURE

For this project, all samples were synthetic commercially grown quartz. The pure Z-growth lumbered bars were obtained from the Sawyer Research Products (14) and Toyo Communications Incorporated (15). From these quartz bars, rectangular Z-plate samples were cut 3mm thick, 15mm long by 10mm wide. The samples were then polished to an optical finish. The samples were identified according to the notation of Markes and Halliburton (16). Using this notation a sample was identified according to grade, Special Premium Q (SP), Premium Q (PQ) or Electronic Grade (EG), according to the bar, A, B, C, etc. and according to the sample number 1, 2, 3 etc. For example, sample EGB12 would be the 12th sample cut from the Bth bar of Electronic Grade quartz.

The grade of quartz is determined by measurement of the optical Q of the crystal. The optical Q value is determined by room temperature infrared transmittance measurements. The optical Q is calculated from the ratio of the transmittance at 3500 cm^{-1} to that at 3800 cm^{-1}. The minimum Q values for SP, PQ and EG quartz are respectively 3 million 2.2 million and 1.8 million.

The SP quartz had the lowest aluminum defect concentration with approximately 1 ppm relative to the silicon atoms. The EG quartz had the highest aluminum defect concentration with 5 to 15 ppm. The PQ quartz is between SP and EG with a concentration of 5 to 8 ppm. These

concentration values are found from IR, ESR and chemical analysis techniques (9). The defect concentration values are only approximate and vary with each bar of quartz.

Preparing Samples for the Sweeper

After the sample was cut and polished it was thoroughly cleaned. Then it was placed in the vacuum evaporation unit. The vacuum evaporation unit is used to deposit NaCl, LiCl or gold films on the sample. For the alkali sweeps, the salt is deposited on only one surface of the crystal, followed by a film of gold on both sides. The salt films provided an ion source for electrodiffusion and the gold film acted as an electrode. The sample was mounted on a movable fixture which was rotated over the correct filament as needed. The alkali salts are placed in a tungsten boat. As the boat is heated the salts evaporated and were deposited on the quartz. The gold film was produced when a current is passed through a tungsten filament which has a gold wire wrapped around it. The gold evaporates from the heated filament and is deposited on the quartz plate. Each of the evaporations were carried out at pressures of 5×10^{-6} Torr. This vacuum reduces contamination of the sample.

For samples that were to be hydrogen swept, only gold films were deposited on each side of the sample. The gold film ensures good electrical contact and an equipotential surface.

Sweeping Apparatus

After the samples have been cut, polished, cleaned and plated they are placed in the electrodiffusion (sweeper) furnace. Figure 1 is a

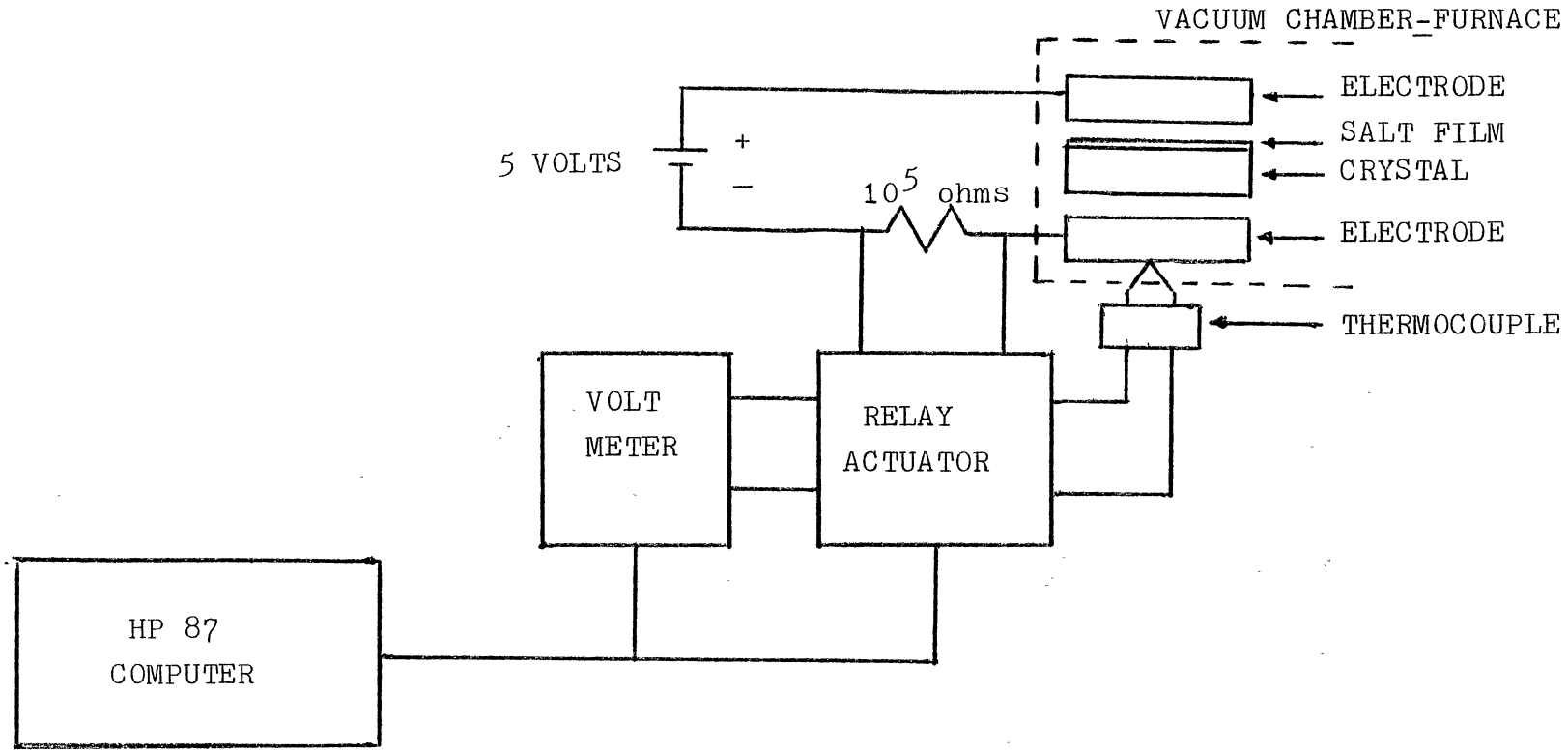

Figure 1. A Block Diagram of the Sweeping Apparatus used in Alkali Sweeps is Shown. The Same Apparatus is used for Hydrogen Sweeps Except the Vacuum is Replaced by a Hydrogen Atmosphere.

block diagram of the sweeper set up for an alkali sweep. The sample is placed between two graphite electrodes and then inserted into a temperature controlled tube furnace. The graphite electrodes are connected in series with a 5 volt power supply and a precision 10,000 ohm resistor. The sample current was measured by using a KEITHLY 192 digital voltmeter to monitor the voltage drop across the resistor. A chromel-alumel thermocouple is used to measure the sample temperature. A HP computer controlled relay box was used to connect the voltmeter to the thermocouple or the precision resistor. A HP 87 microcomputer was used to record the voltmeter readings. The furnace temperature is controlled by a DATA TRAK card programmable temperature control unit. As the temperature of the furnace is lowered the HP 87 records the sample current and the temperature. With the help of additional software this data is converted into a plot of the log of the products of conductivity and temperature versus 1000/T. The activation energy and preexponential factor are determined by a least squares analysis of the data.

The hydrogen sweeps required the apparatus to be modified slightly. The 5 volt power supply used in the alkali sweeps was replaced by a high voltage KEPCO power supply. The voltage across the sample was increased from 5 volts to 800 volts. Higher voltages are needed because the hydrogen ions have a lower mobility in quartz than the Li^+ or Na^+. The resulting electric fields for the hydrogen sweeps were typically 2700 volts/cm. The partial vacuum required for the alkali sweeps is replaced by a hydrogen atmosphere. The sample current and temperature were measured in the same way as in the alkali sweeps. From this temperature and current data the conductivity is calculated by the HP 87.

By adding a digital programmable power supply to drive the KEPCO power supply the dependence of the hydrogen ion current density upon electric field can be measured. With the furnace temperature held constant the applied voltage across the sample is lowered from 800 volts to 0 volts in steps of 50 volts. The current density and electric field are calculated and stored by the HP 87 computer.

Program SIGTEMP3 is used in both alkali and hydrogen sweeps to record the conductivity data. Figure 2 is a flow chart of the SIGTEMP3 program. The HP 87 microcomputer stores the conductivity versus temperature data on a floppy disk. Program SIGPLOTR3 is used to analyze the conductivity versus temperature data. This program then plots log conductivity times T versus 1000/T. In the ideal case of only one conduction mechanism this plot should be a straight line. Program SIGPLOTR3 has a least squares routine to determine the slope (activation energy) and intercept (preexponential factor).

Infrared Absorption Measurements

Before and after each alkali or hydrogen sweep the infrared absorption spectrum was measured using a Beckman 4240 spectrophotometer. The sample was mounted inside a liquid nitrogen optical dewar that has CaF_2 windows. A thermocouple is mounted on the sample holder cold finger. This allowed the sample temperature to be monitored during the infrared measurement. If the sample temperature is not held near 77K the absorption peaks begin to broaden. IR runs are usually made from 3700 to 3000 cm^{-1} where the OH^- stretching mode is active. The samples are mounted so that the light is incident perpendicular to the crystal surface. This orientation results in the electric field

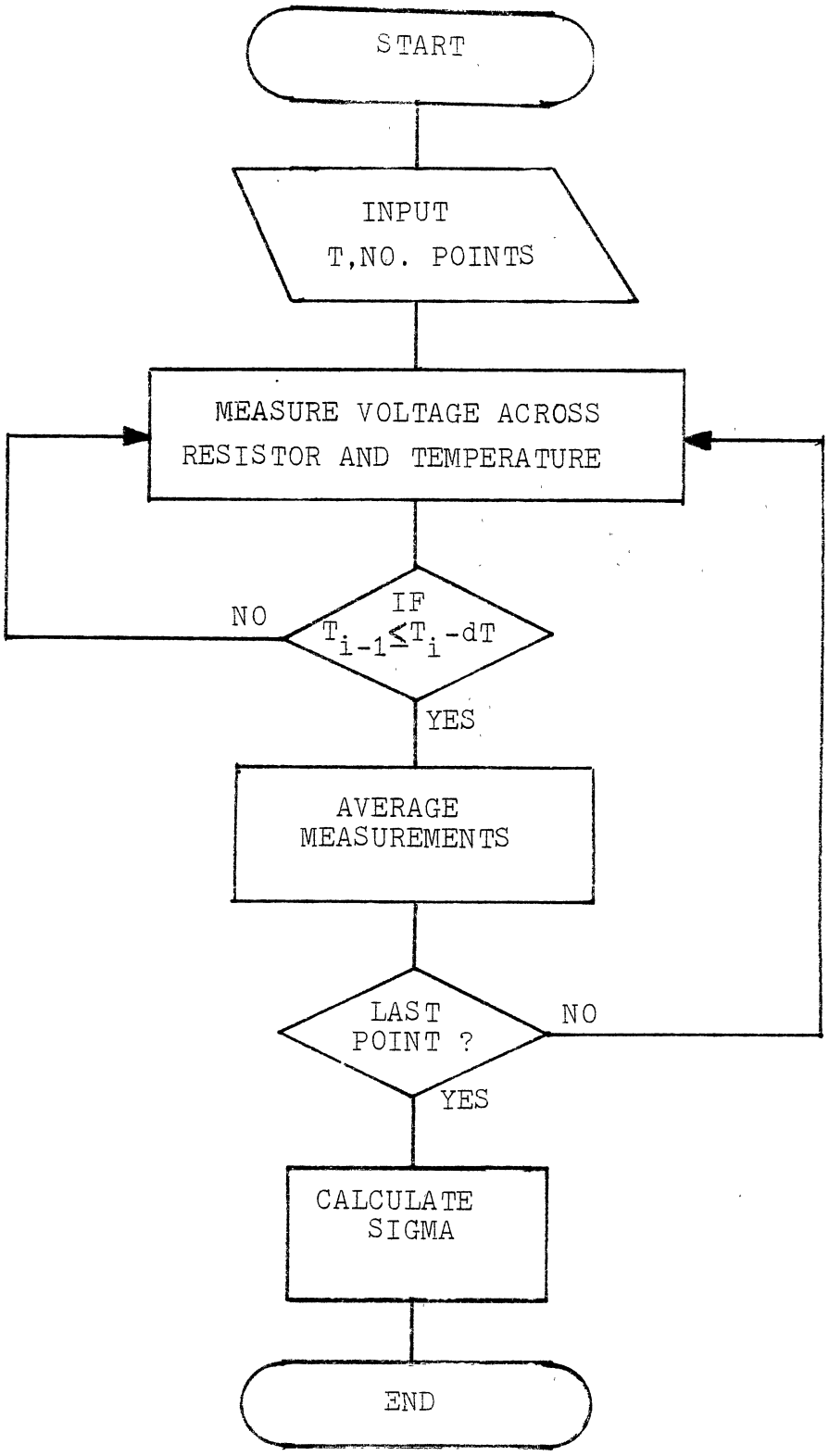

Figure 2. Flow Chart of the SIGTEMP3 Program is used in the Acquisition of Conductivity Versus Temperature Data.

vector of the light being perpendicular to the C axis of the crystal. This IR data is used to determine the relative hydrogen concentration in each sample.

Error Analysis

Errors in temperature measurements are present because of the inaccuracies of the thermocouple and because a complete thermal equilibrium may not be reached between the sample and furnace. The inaccuracy in temperature is believed to be less than ±2 C°. As each hydrogen sweep progressed the KEPCO power supply voltage drifted by about 1 percent. This will cause a small error in the calculation of the conductivity. From the Arrhenius plot the activation energy is calculated, on several sweeps the conductivity data was slightly curved. This curvature is probably the result of more than one conduction mechanism. The program used to calculate the preexponential factor and activation energy does not take into account the change in slope. As a result of this deviation from a straight line, errors in the calculation of the activation energy and preexponential factor are introduced. The preexponential factor is calculated by exponentiation of the y intercept found from the least squares routine. The use of the exponential function in calculating the preexponential factor caused larger errors than in the linear calculation of the activation energy. This course of error varies with each sweep. The deviation from a straight line is more apparent in the EGB quartz than the SPA or PQI.

CHAPTER III

RESULTS AND DISCUSSION

A series of electrodiffusion runs (sweeps) were carried out on three different grades of synthetic quartz; SP, PQ and EG. The sweeping runs were made over the temperature range of 350°C to 530°C. Three types of ions were used for the sweeps, these were Li^+, Na^+, and H^+. As a result of these sweeps the dependency of the activation energy, pre-exponential factor and conductivity was measured using the three different mobile ions in the three different grades of quartz.

Before the conductivity can be measured the current through the sample must be constant. When the potential is applied across any of the samples there is a initial current surge (2). This surge is due primarily to trapped ions in the crystal that are swept out. Figure 3 is a typical plot of current versus time after the initial application of the potential. As Figure 3 illustrates the lower voltage for the alkali sweeps resulted in a much lower initial current. For all sweeps the current had reached a steady value after 50 minutes. After the current was stable the temperature of the sample could be programmed down and the current recorded as a function of temperature. The conductivity and its' activation energy and preexponential factor were calculated from this data.

To monitor the concentration of the $Al\text{-}OH^-$ centers in the crystals an infrared spectrum at liquid nitrogen temperature was recorded before

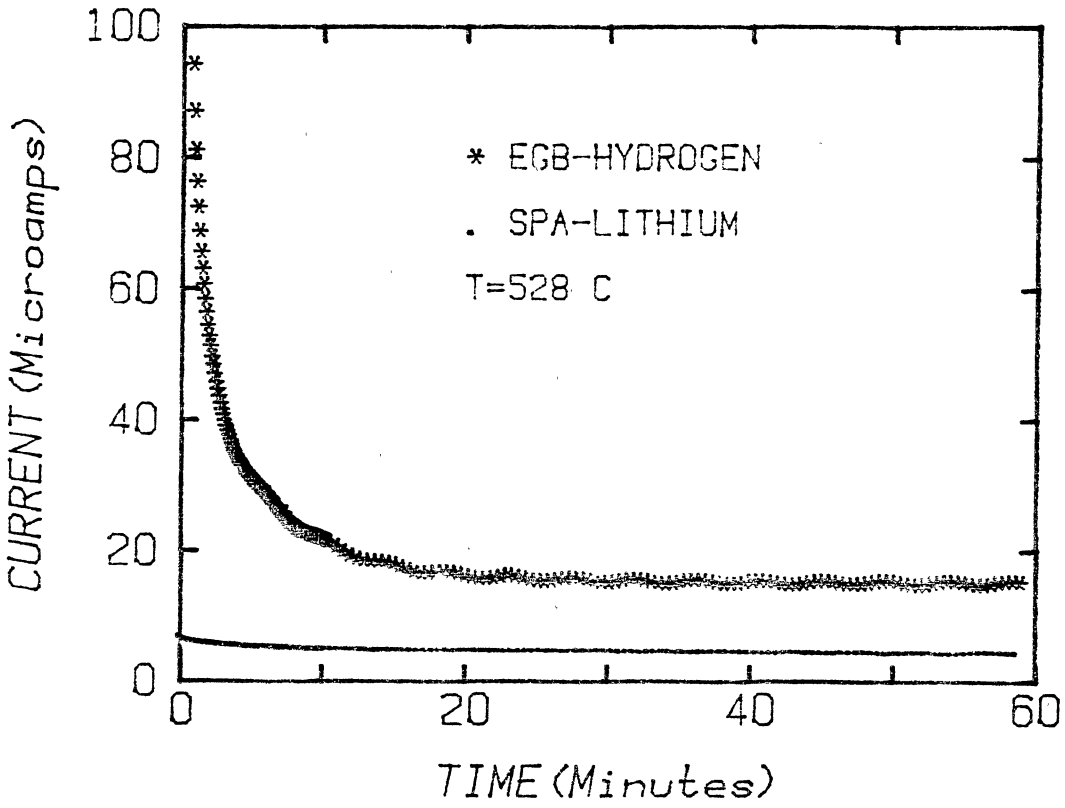

Figure 3. The Application of a Voltage Across the EGB Sample Causes an Initial Surge Current. This Initial Surge Current is Short Lived, a Steady State Current is Reached Within 20 Minutes.

and after each sweeps. Figure 4a is a spectra of the SPA sample before any sweeps. The height of the 3306 and 3367 cm^{-1} peaks are proportional to the total $Al\text{-}OH^-$ concentration. There is no 3367 or 3306 cm^{-1} signal above the noise level in the as-received spectrum shown in Figure 4a.

During the course of the investigation the SPA sample was subjected to ten separate electrodiffusions. The four initial electrodiffusions consisted of two sodium sweeps followed by two lithium sweeps. In Figure 5 two plots of σT versus 1000/T for sodium ions in SP quartz are shown. Figure 6 shows similar plots for lithium and hydrogen ion electrodiffusion in SP quartz. The smaller lithium ion is more mobile in quartz resulting in a slightly higher conductivity. The activation energies were nearly equal with .79 eV for sodium and .76 eV for lithium. A complete listing of the average activation energies and preexponential factors are listed in Table 1. After these four alkali sweeps the SPA sample was swept twice in a hydrogen atmosphere. The conductivity for the hydrogen sweeps was lowered by a factor of 2000 from the alkali sweeps. The activation energy for the hydrogen sweep increased to 1.76 eV in the SPA sample. Since the conductivity is proportional to the negative exponential of the activation energy, the higher activation energy for hydrogen results in the lower conductivity. After these two hydrogen sweeps the IR spectra was again recorded. Figure 3b shows the spectra after the introduction of hydrogen into the sample. A small number of $Al\text{-}OH^-$ centers were produced by the hydrogen electrodiffusions as shown by the small 3367 and 3306 cm^{-1} bands.

After the four initial alkali sweeps and the two subsequent hydrogen sweeps the SPA sample was swept four more times by alkali

SPA Quartz

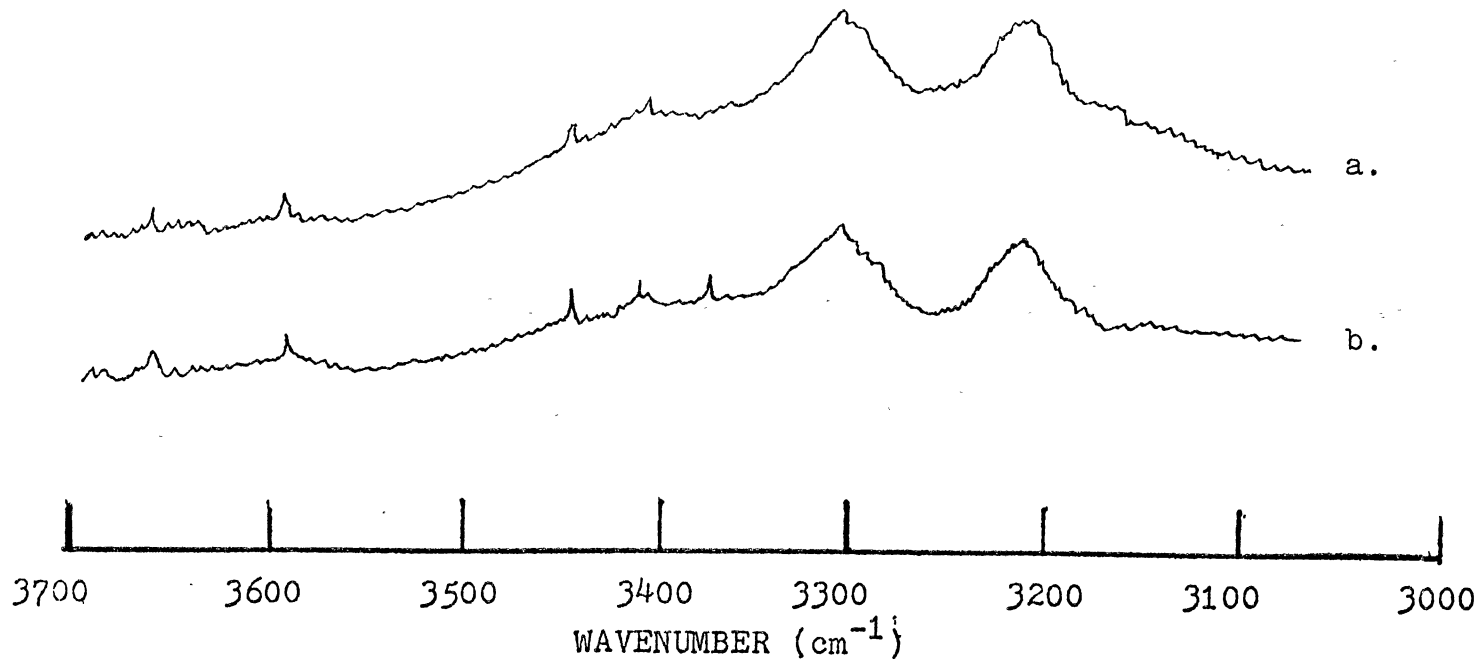

Figure 4. The infrared Spectra of SPA Quartz is Shown Before (a) and after (b) a Hydrogen Electrodiffusion.

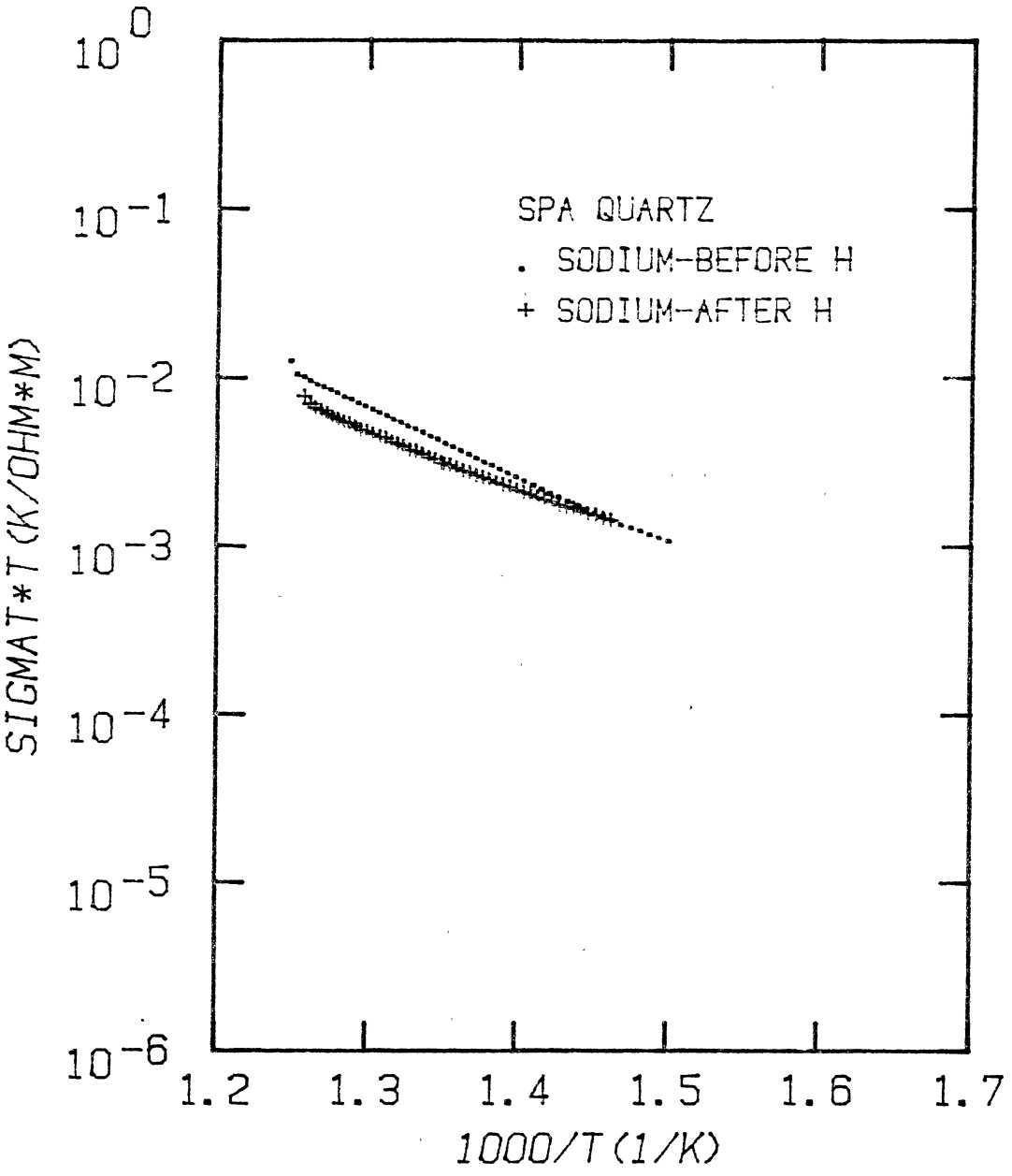

Figure 5. A Plot of the Conductivity Temperature Product Versus 1000/T for SPA Quartz is Shown for a Sodium Run.

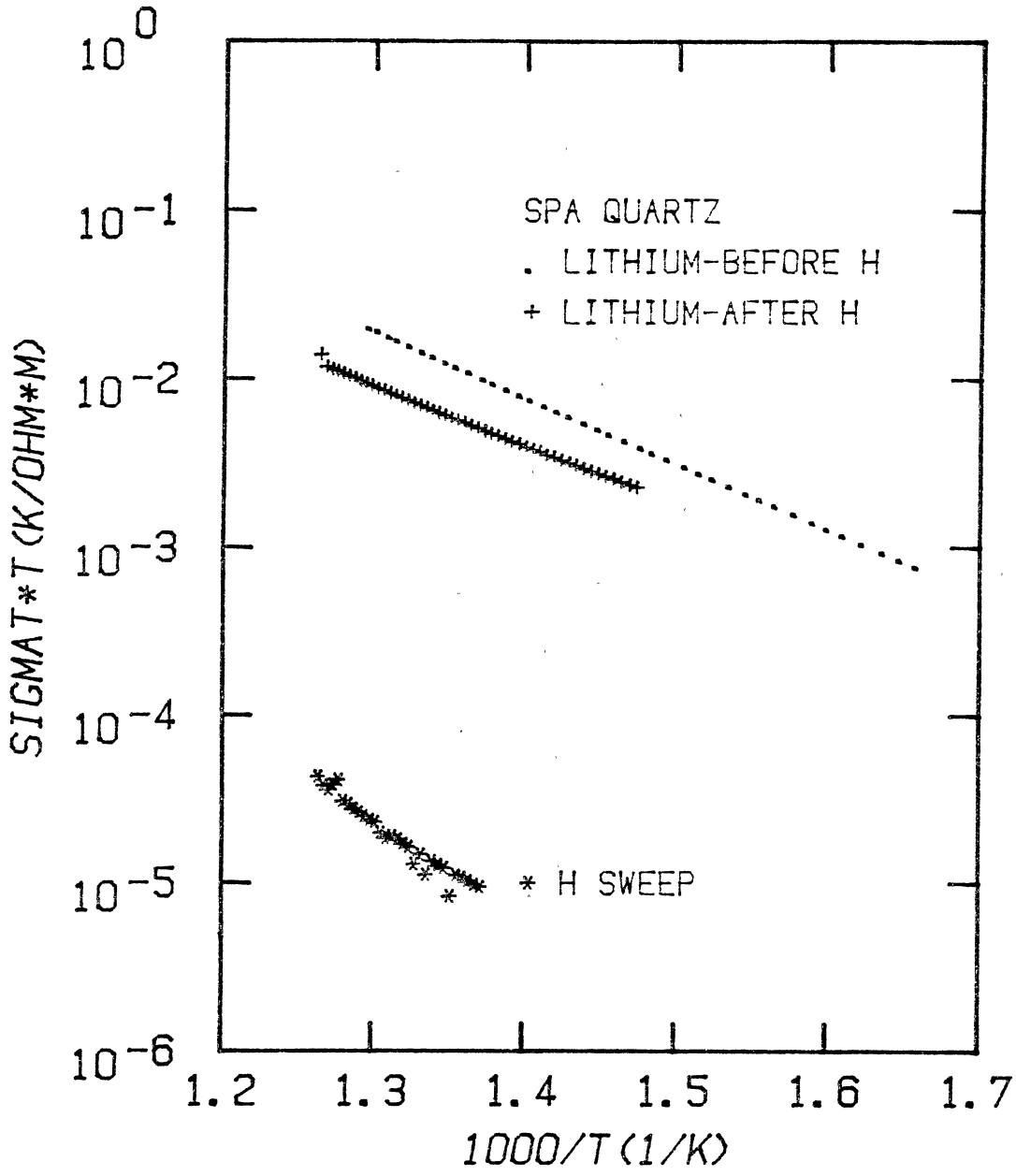

Figure 6. A Conductivity Versus Temperature Plot for SPA Quartz. The Two Upper Plots are for Lithium Sweeps, the Lower Curve is for a Hydrogen Sweep.

TABLE I

ELECTRODIFFUSION DATA SUMMARY

Sample Name	Mobile Ion	Average Activation Energy E_a(eV)	Average Preexponential A(K/ohm-cm)
		BEFORE HYDROGEN SWEEP	
SPA	Lithium	.76	21-22
PQI	Lithium	.72-.73	17
EGB	Lithium	1.13	15E3
SPA	Sodium	.79	13
PQI	Sodium	.78	12
EGB	Sodium	1.12	3500
		HYDROGEN SWEEP	
SPA	Hydrogen	1.17	48
PQI	Hydrogen	1.35	190
EGB	Hydrogen	1.76	2E5
		AFTER HYDROGEN SWEEP	
SPA	Lithium	.71	3.8
PQI	Lithium	.71	4.1
EGB	Lithium	1.0	560
SPA	Sodium	.66	.8
PQI	Sodium	.74-.75	3.8
EGB	Sodium	.33	3E-3

ions. Two sweeps for sodium and lithium each. The results of the sweeps are shown in Figures 5 and 6. The conductivity was reduced by approximately a factor of two from that of the initial alkali runs. This lowering of the conductivity is a result of the previous hydrogen sweeps. The hydrogen electrodiffusion caused most of the aluminum defect traps to be associated with hydrogen ions. As illustrated by the infrared spectras, Figure 4b, the hydrogen ion concentration is not effected by the low electric field alkali sweeps. The trapped hydrogen lowers the number of traps available for the alkali ions. By lowering the number of available carrier ions the conductivity is lowered. Since the hydrogen fills the deeper energy aluminum traps the activation energy is lowered. The activation energy for lithium, after the hydrogen sweeps, was lowered from .76 eV to .71 eV. The activation energies for the sodium sweeps was also lowered. After all ten sweeps had been completed on the SPA sample the IR spectra was again recorded. The four final alkali sweeps had no effect on the Al-OH concentration in the quartz. The final spectra was identical to the spectra shown in Figure 4b.

The next sample to receive the same series of sweeps was the PQI sample. Due to the PQI sample having approximately the same Aluminum defect concentrations as the SPA sample the IR spectras are virtually identical. The conductivity versus temperature data is presented in Figure 7. The average activation energy for the lithium sweep was .72 eV and .78 eV for the sodium. The conductivity for the sodium was about 10 to 20 percent lower than the lithium. After these four alkali sweeps the PQI sample was swept twice in a hydrogen atmosphere. The conductivity was again lowered by a factor of 2000 from the alkali

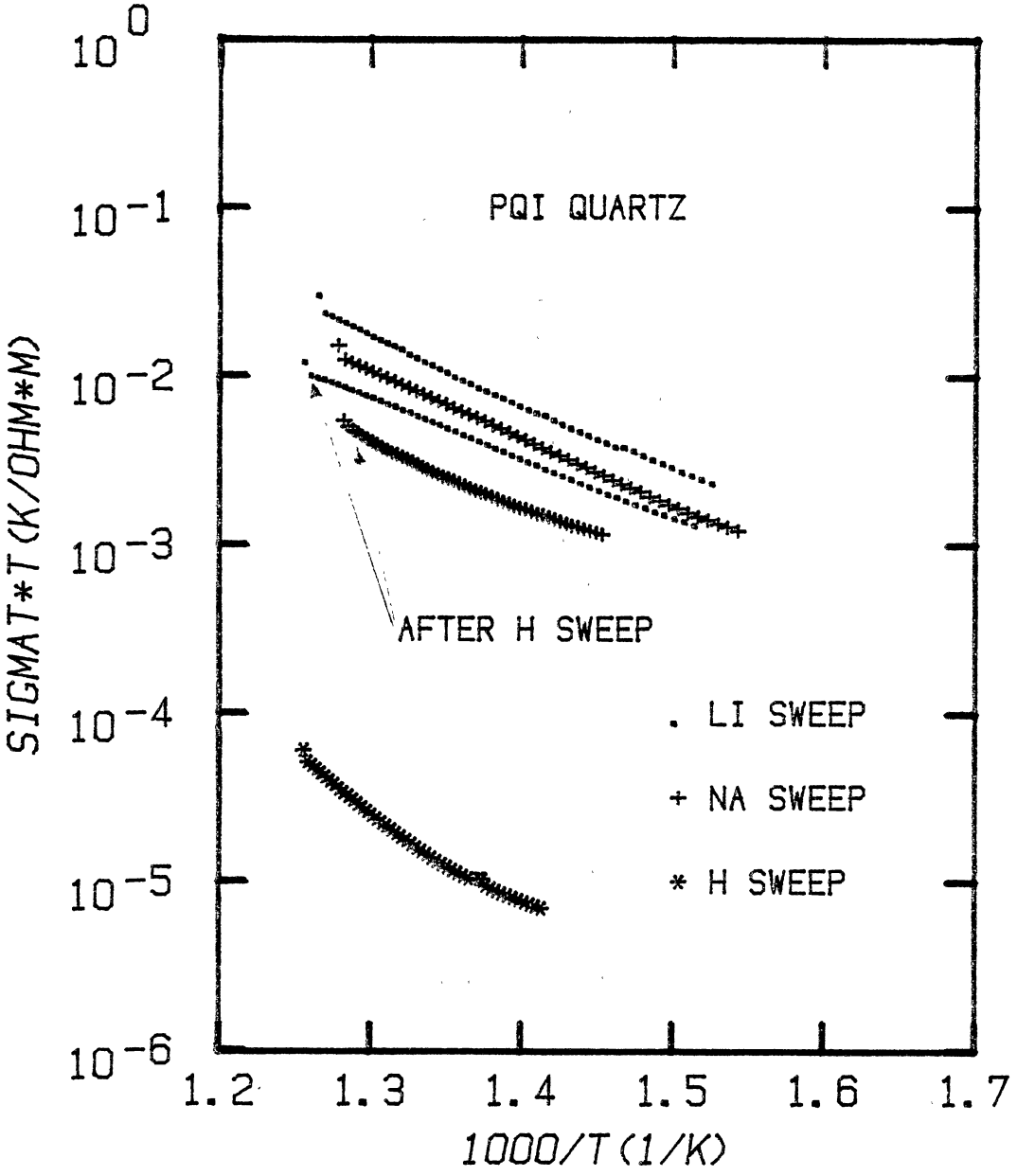

Figure 7. Five electrodiffusions for Sodium, Lithium and Hydrogen in PQI Quartz are Plotted. Two of the Plots Show the Effects of the Hydrogen Sweeps Upon Subsequent Alkali Sweeps.

sweeps. The average activation energy was 1.35 eV for the hydrogen sweeps. The Arrenhnius plot for the hydrogen data showed a small curvature. As the temperature decreased the slope (activation energy) of the line decreased. The curvature is attributed primarily to other defect centers and carrier ions acting in parallel. Some of the curvature is a result of leakage currents and offsets in the voltmeter. As in the SPA sample, the hydrogen sweeping of the PQI sample caused an increase in height of the 3306 and 3367 cm^{-1} peaks. After these two hydrogen sweeps the PQI sample was subjected to four additional alkali sweeps. Figure 7 shows the conductivity data for one each of the lithium and sodium sweeps. As in the case of the SPA the conductivity for both sodium and lithium was lowered by a factor of approximately 2. There was a slight lowering (about 5 percent) of the activation energy and the preexponential factor in both types of sweeps. As a whole, the sweeping results for the PQI sample was very similar to the SPA sample. This is a direct result of the similarity in aluminum defect concentration of the two samples, as determined by the IR spectra of the samples.

The final sample studied was the EGB quartz. This sample had a higher aluminum defect concentration than either the SPA or the PQI sample. Figure 8a shows the IR spectra for the as received EGB. There are three prominent peaks at 3585, 3437 and 3400 cm^{-1}, these are associated with impurities other than the aluminum. The two broad absorption peaks at 3300 and 3200 cm^{-1} are intrinsic peaks to quartz. Five of the conductivity plots for the EGB quartz are shown in Figure 9. The initial sodium sweeps resulted in an average activation energy of 1.2 eV and preexponential factor of 3500 (K/ohm-cm). The lithium

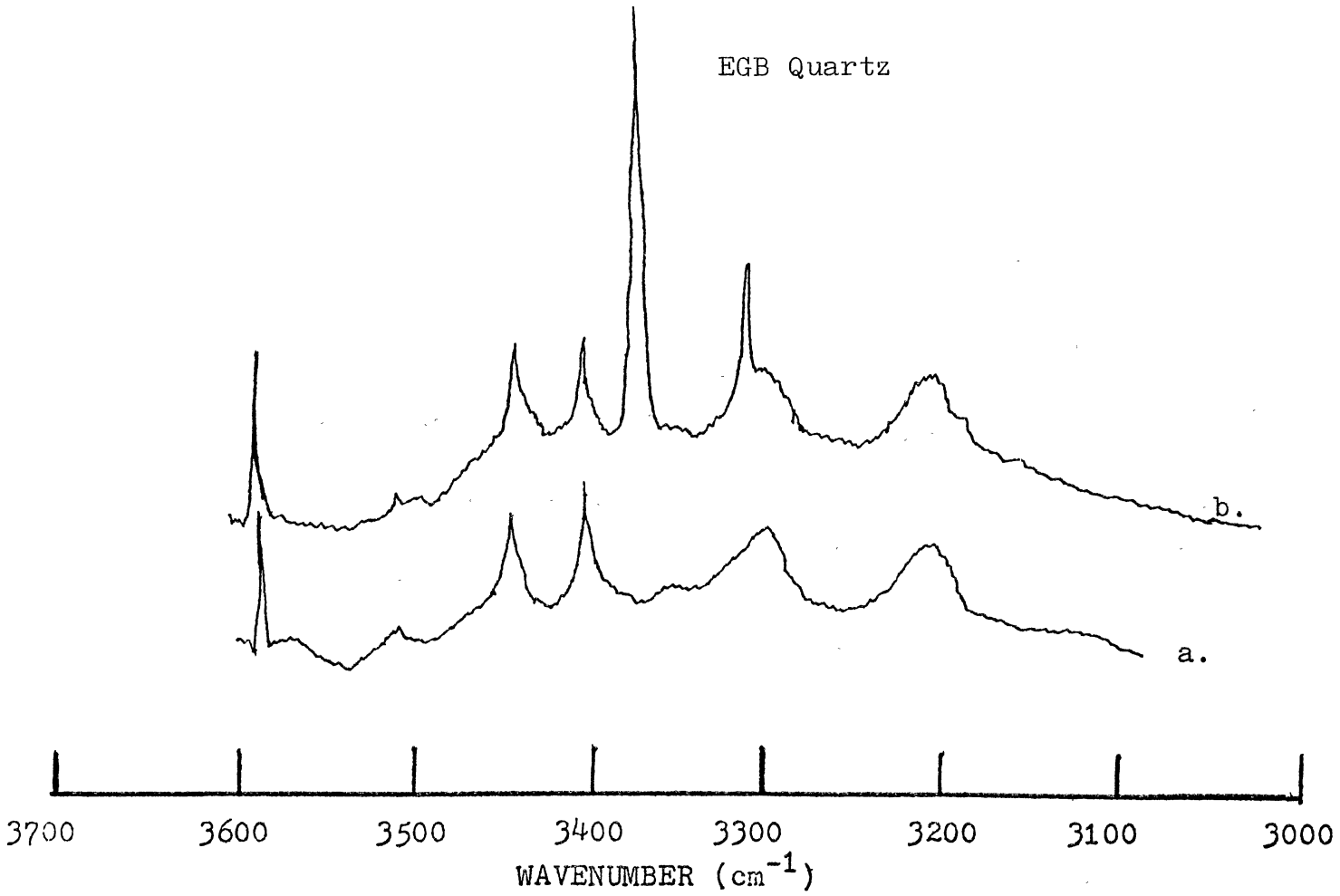

Figure 8. Two Infrared Spectra for EGB Quartz are Shown. The a. Plot is for As-Received Quartz, the b. Plot is after a Hydrogen Sweep.

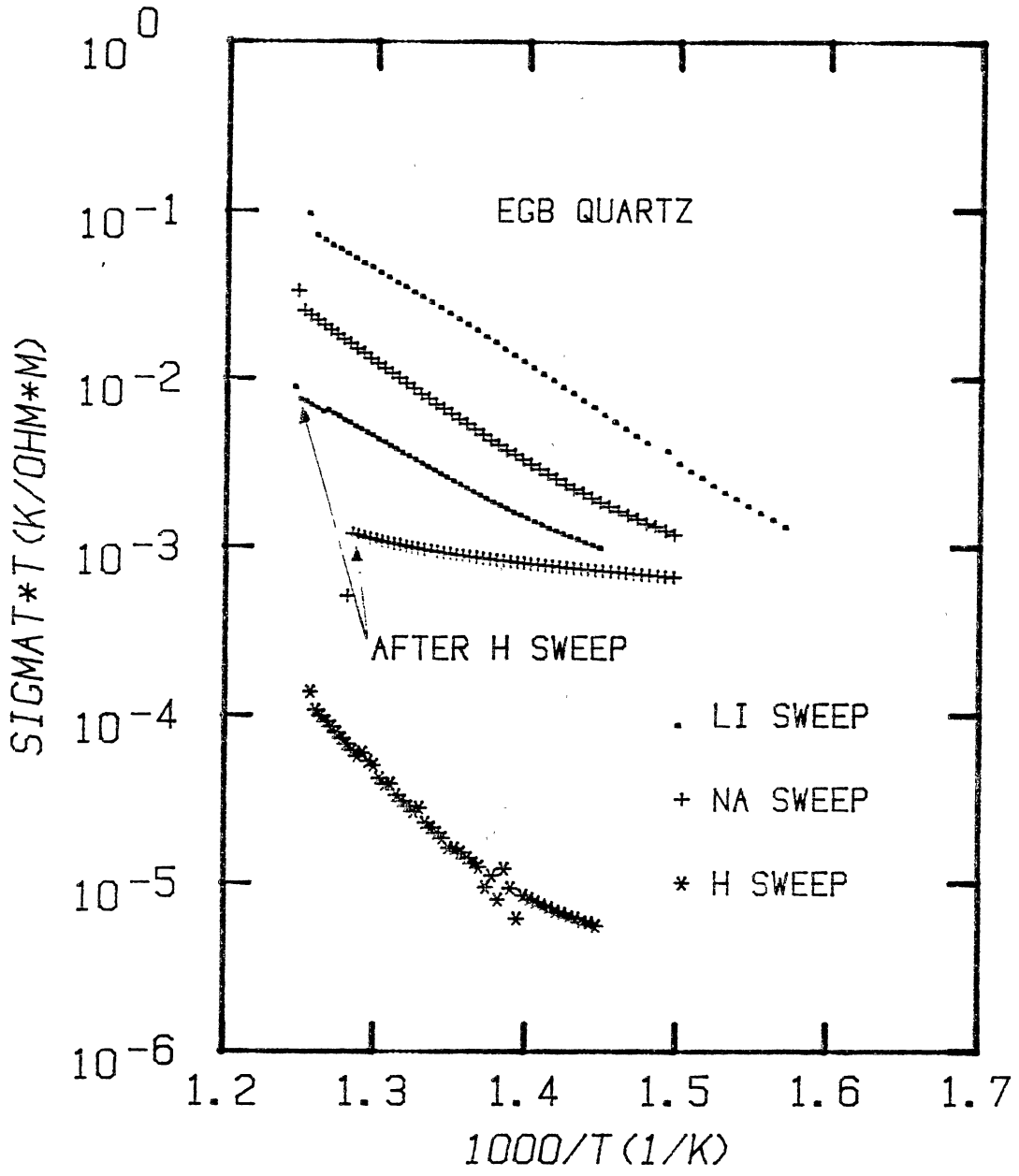

Figure 9. Five Electrodiffusions in EGB Quartz with Sodium, Lithium, and Hydrogen as the Mobile Ions are Shown. The Upper Four Plots are for Alkali Sweeps, the Lower Plot is for Hydrogen.

sweeps resulted in an average activation enegy of 1.13 eV and a pre-exponential factor of 15,000 (K/ohm-cm). These are consistant with the trend of a slightly lower activation enegy for lithium. These activation energies are about 50 percent higher than for the PQI or SPA samples. After the four initial alkali electrodiffusions the EGB sample was swept twice in a hydrogen atmosphere. The conductivity was again lowered by a factor of greater than 2000. The hydrogen conductivity data showed a little more curvature toward a lower activation energy than in the SPA or PQI samples. The four final alkali sweeps followed the two hydrogen sweeps. The hydrogen sweeps had a more pronounced effect on the EGB alkali activation energies than in the two previous samples. For the lithium case the activation energy was lowered by .13 eV, from 1.13 eV down to 1.00 eV. The activation energy was also lowered for the sodium case. The preexponential factor for the sodium ions went from 3500 (K/ohm-cm) before the hydrogen sweeps to less than 1(K/ohm-cm) after the introduction of hydrogen. The conductivity for both the sodium and lithium ions decreased by a factor of nearly 10. As shown by Fig. 8b the introduction of hydrogen caused a large increase in absorption peaks at 3306 and 3367 cm^{-1}. The four final alkali sweeps caused no change in these absorption peak heights.

Figure 10 is a plot of lithium and hydrogen sweeps in each type of quartz. In both cases, lithium and hydrogen, the conductivity, activation energy and preexponential factor are higher than in the SPA or PQI samples. The overlapping conductivity plots for the PQI and SPA samples indicate their similarity in aluminum concentration. Figure 11 shows a comparison of sodium sweeps in the three different types of quartz. The EGB sample has the higher activation energy and preexpon-

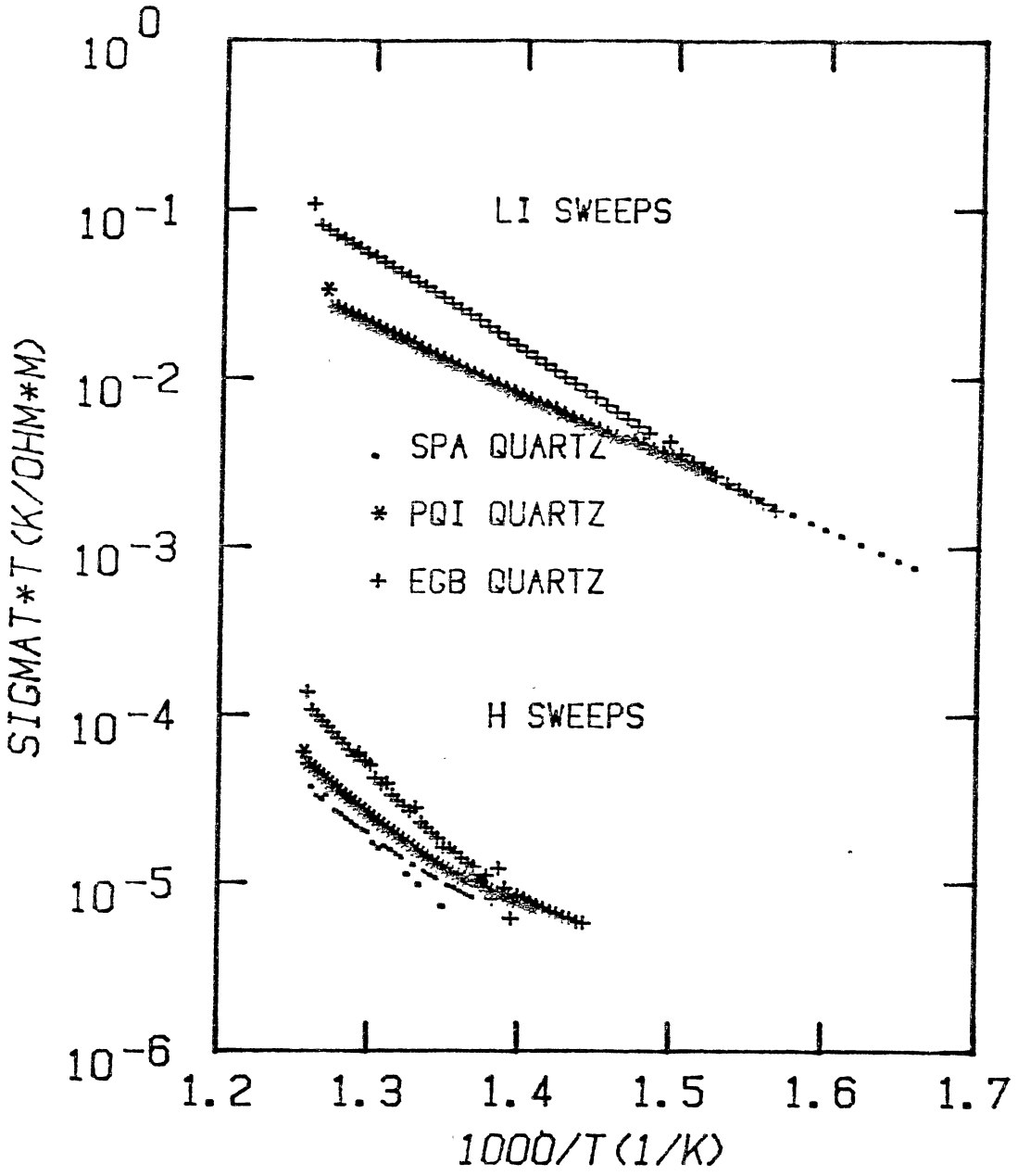

Figure 10. A Comparison of Lithium and Hydrogen Sweeps in SP, PQ, and EG Quartz is Shown.

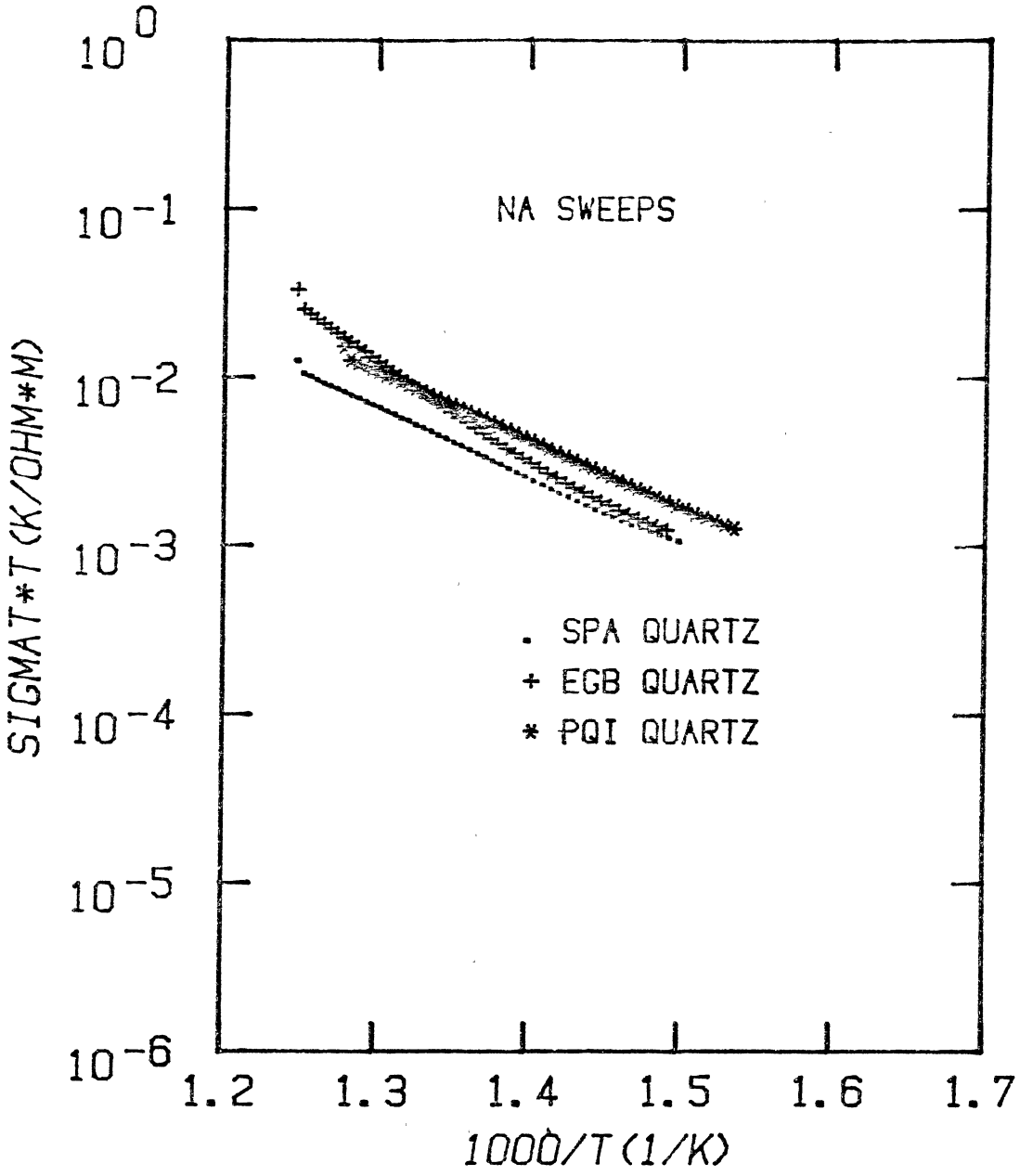

Figure 11. Three Electrodiffusions of Sodium Ions in SP, PQ, and EG Quartz are Shown.

ential factor compared to the SPA and PQI. The PQI and SPA samples do not show any overlap as they did in the lithium sweeps.

The ionic conductivity of quartz has been studied by several researchers in the last 30 years. Their experimental apparatus and results have been similar. Verhoogen (17) in 1952 found the activation energy for a lithium ions in quartz to be .89 eV and 1.04 eV for sodium. The samples studied were natural quartz, not the synthetic quartz used in this study. The applied fields were much higher (greater than a factor of 20) than the fields used in this experiment. Also Verhoogen swept his quartz with salt films in an air atmosphere, this introduced a small hydrogen current into the results. In 1957 Wenden (2) conducted an extensive investigation into the ionic conductivity of quartz. These sweeps were done with natural quartz in air. He measured the activation energy for sodium ions in quartz to be 1.04 eV. Snow and Gibbs (18) determined the activation energy for sodium and lithium in quartz by a.c. measurements of the dielectric constant. The quartz was first swept by sodium and lithium in a d.c. field, then from dielectric constant versus frequency and temperature measurements the activation energy was determined. For both sodium and lithium ions the activation energy was found to be .72 eV. The most recent work in this area has been done by Nowick (5). His measurements are for a.c. conductivity in synthetic quartz. These activation energies are based on all of the free ions present in the as received quartz. For as received PQ quartz the activation energy was 1.33 eV, for as received EG quartz the activation energy was 1.4 eV. After sweeping the quartz in a hydrogen atmosphere he records the activation energy as 1.38 eV. This value differs by only 2 percent from the d.c. value presented in this thesis.

Figure 12 is a plot of the current density versus electric field for a hyrogen sweep in SPA quartz. Figure 12 indicates that quartz does obey Ohm's law (2) up to approximately 3000 v/cm. As the temperature is increased to 534°C the SPA quartz deviates from Ohms law at 2500 v/cm. This is consistant with the fact that as the temperature increases more carriers become available. By measuring the slope of the T = 534°C line and taking the physical dimensions of the SPA sample into account a resistance of 157 megaohms is obtained. For the EGB sample at T = 532°C the resistance is 52 megaohms. The resistance is inversely proportional to the aluminum concentration and the sample temperature.

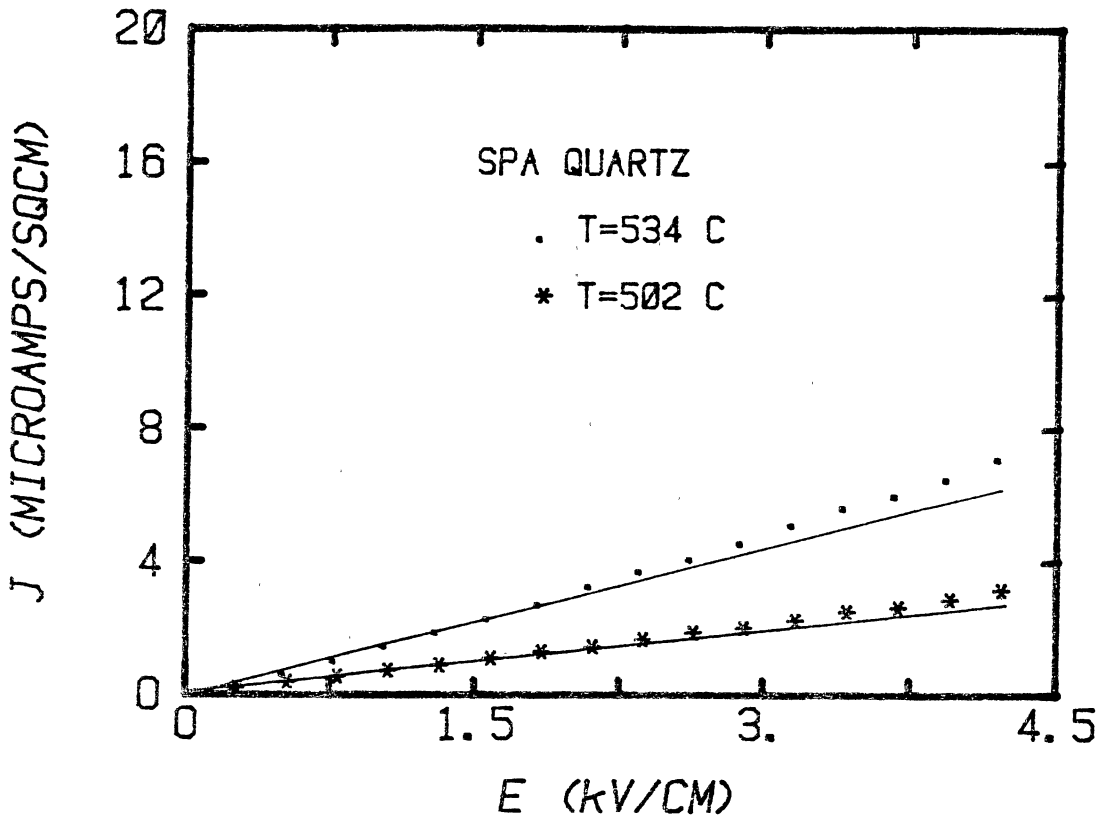

Figure 12. A Plot of the Current Density Versus the the Applied Electric Field in SPA Quartz at 502 C and 534 C. Note the Ohmic Behavior up to about 2 KV/cm.

CHAPTER IV

CONCLUSIONS

From the results of this investigation four main conclusions can be drawn about the ionic conductivity of synthetic quartz. As a result of the curvature of the Arehnius plots we conclude that there is more than one defect center involved in the conduction of ions in quartz. Secondly, that the electrodiffusion of alkali ions does not have an appreciable effect on the Al-OH^- concentration. Third, the sweeping of hydrogen ions does cause a decrease in the activation energy and conductivity in subsequent alkali sweeps. Finally, the relationship between aluminum defect concentration and the associated activation energy and conductivity is shown.

Electrodiffusion has proven to be a very effective method of exchanging charge compensating ions at aluminum defect centers in quartz.

REFERENCES

1. G. Spezia, Atti. Acad. Torino 44, 95 (1908).

2. H. E. Wenden, The American Mineralogist 42, 859 (1957).

3. Handbook of Chemistry and Physics, 56th Edition, CRC Press, (1975-76).

4. J. A. Weil, Radiation Effects 26 (1975) 261.

5. H. Jain and A. S. Nowick, J. Appl. Phys. 53, 477 (1982).

6. A. Kats, Philips Res. Repts. 17, 201 (1962).

7. A. Kats, Philips Res. Repts. 17, 133 (1962).

8. S. P. Doherty, J. J. Martin, A. F. Armington, R. N. Brown, J. Appl. Phys. 51, 4164 (1980).

9. L. E. Halliburton, N. Koumvakalis, M. E. Markes and J. J. Martin, J. Appl. Phys. 52, 3565 (1981).

10. D. B. Fraser, Physical Acoustics, 5, 59, Academic Press, N.Y. (1968).

11. K. L. Yip and W. B. Fowler, Phys. Rev. B11, 2327 (1975).

12. A. B. Lidiard Hand. of Phys. 20, 246 (1957).

13. M. V. Lomonosov Soviet Physics, Crystallography 13, 540 (1969).

14. Sawyer Research Products Inc., 35400 Lakeland Blvd., Eastlake, Ohio, 44094.

15. Toyo Communications Equipment Company, Kawasaki, Japan.

16. M. E. Markes and L. E. Halliburton, J. Appl. Phys. 50, 8172 (1979).

17. J. Verhoogen, Am. Mineral, 37, 637 (1952).

18. E. H. Snow and P. Gibbs, J. Appl. Phys. 35, 2368 (1964).

VITA

Jerry Douglas West

Candidate for the Degree of

Master of Science

Thesis: ELECTRODIFFUSION OF LITHIUM, SODIUM AND HYDROGEN IONS IN SYNTHETIC QUARTZ

Major Field: Physics

Biographical:

Personal Data: Born in Springfield, Missouri, February 23, 1959, the son of Jerry and Marie West.

Education: Graduated from Logan-Rogersville High School in 1977; attended Southwest Missouri State University during 1977 and 1978; Graduated with a Bachelor of Science degree from the University of Missouri-Rolla in 1980; completed requirements for the degree of Master of Science at Oklahoma State University, Stillwater, Oklahoma in July, 1984.